The use of remote sensing tools for accurate charcoal kilns' inventory and distribution analysis: Comparative assessment and prospective

Cláudia Oliveira, Stéphanie Aravecchia, Cédric Pradalier, Vincent Robin, Simon Devin

International Journal of Applied Earth Observations and Geoinformation 105 (2021) 102641

Contents lists available at ScienceDirect

International Journal of Applied Earth Observations and Geoinformation

journal homepage: www.elsevier.com/locate/jag

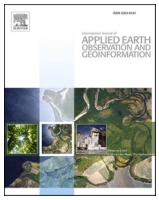

The use of remote sensing tools for accurate charcoal kilns' inventory and distribution analysis: Comparative assessment and prospective

Cláudia Oliveira [a,*], Stéphanie Aravecchia [b], Cédric Pradalier [b], Vincent Robin [a], Simon Devin [a]

[a] LIEC, University of Lorraine, CNRS, Metz, France
[b] IRL 2958 Georgia Tech – CNRS, Metz, France

ARTICLE INFO

Keywords:
Charcoal kiln
LiDAR
Automatic detection
Spatial analysis
Deep learning

ABSTRACT

Historical charcoal production is one of the significant factors affecting today's forest dynamics. A key challenge is to develop tools to investigate historical charcoal production over large areas, allowing a more comprehensive understanding of past impacts and history of charcoal production over a given landscape. In this study, high-resolution remote-sensing airborne LiDAR images over a large woodland area were used to compare manual on-screen versus algorithm-based automatic methods to inventory charcoal kilns with inputs of field-validated data. The results revealed that (1) the on-screen detection method provided less false-positives, (2) the automatic method detects a higher number of kilns and (3) kiln distribution seemed to be connected mostly to land ownership rather than to environmental variables. This study validates a new method of charcoal kilns' inventory and spatial analysis that can be applied to other areas to better understand the effect of past biomass harvesting for charcoal production on forest dynamics.

1. Introduction

In Europe, charcoal produced from biomass exploitation was a key source of energy for the (proto-) industrial development from the Middle-Ages to the emergence of fossil energy sources during the 19th century (Pain, 2017; Smil, 2004). The analyses of single relict sites of charcoal production (i.e., charcoal kilns or hearths) provide key information about former local forest composition, woodland structure, wood resource management and use (Ludemann et al., 2004; Deforce et al, 2013; Schneider et al, 2020). However, charcoal production was, most of the time, spread over large areas (e.g., Ludemann, 2003, Deforce et al., 2020), and thus the related ancient exploitation of wood resources left long-lasting traces on the environment (Fouédjou et al., 2021) on large spatial scales (Rösler et al., 2012; Carrari et al., 2016). Therefore, quantification and spatial distribution analysis of kilns are crucial to assess the impacts of charcoal production on woodlands (Ludemann et al., 2004; Schmidt et al., 2016; Schneider et al., 2020). Nevertheless, field prospection of these structures was found to ignore a large - number of kilns even in extensively studied areas (Ludemann, 2012). Moreover, the prospection and fieldwork to achieve a complete overview of kiln distribution are time-consuming. Therefore, most studies about kilns focus on few investigated sites at local (Nelle, 2003) or small catchment scales (Gocel-Chalté et al., 2020). The emergence and increasingly more detailed airborne LiDAR (Light Detection and Ranging) data provide a powerful tool to obtain more precise data on kiln density and distribution over large areas. LiDAR images have been used for more than a decade to map archaeological structures (e.g., Crutchley and Crow, 2010; Chase et al., 2017), including charcoal kilns (e.g., Ludemann, 2012; Raab et al., 2015, Trier et al., 2021). Indeed, charcoal kilns are characterized by a circular to oval outline easily visible in steep slopes in the field (Bonhage et al., 2020(Schneider et al., 2015). When the topography is gentle, there is less requirement to artificially level the surface to build a kiln, making the detection in these areas challenging since there is less contrast between the kiln and the surroundings. Thus, prospecting kilns and other micro-topographical structures in Digital Elevation Models (DEM) can be made more efficient based on hillshade pictures (Raab et al., 2015), derived images such as slope (McCoy et al., 2011) or images under sky-view factor (i.e., "visualization technique based on diffuse light that overcomes the directional problems of hill-shading", Kokalj et al., 2011), principal component analyses or local-relief models (Bennett et al., 2012; Challis et al., 2011; Štular et al., 2012). However, the first proposed methods, appeared to be highly hand-engineered and strongly dependent on the numerical model and therefore may be case-specific.

* Corresponding author at: LIEC/Université de Lorraine, Campus Bridoux, 8 rue du Général Delestraint, 57070 Metz, France.
E-mail address: claudia.oliveira@univ-lorraine.fr (C. Oliveira).

https://doi.org/10.1016/j.jag.2021.102641
Received 29 September 2021; Received in revised form 18 November 2021; Accepted 29 November 2021
Available online 4 December 2021

Methods for the automatic detection of landforms on digital data have emerged over the last decade (Toumazet et al., 2017; Davis 2019; Davis et al., 2019), allowing a significant rise in the analytical capacities. In the last few years, the field of computer vision has been significantly transformed by the development of deep learning algorithms such as Convolutional Neural Networks (CNNs; (Ren et al., 2015)), providing new tools to improve charcoal kiln inventory (Bonhage et al., 2021; Trier et al., 2021).

Here, we present a case study using an innovative approach of inventory of charcoal kilns that combines for the first time both on-screen and algorithm-based detection complemented with field validation on a large area, to assess and explain the spatial distribution of kilns related to socio-environmental territorial attributes. Two detection methods were applied and compared: 1) an on-screen detection and 2) an object detection method, based on the analysis of a DEM. Moreover, it was developed an efficient and easily transferable charcoal kiln detection methodology to another dataset, using standard libraries and Application Programming Interfaces (API) such as TensorFlow (Abadi et al., 2016). The inclusion of a field-validation step was crucial to tune the detection and achieve a solid quantification to obtain an inventory close as possible to reality, which plays a key role when studying the impacts and legacy of historical charcoal production.

2. Methods

2.1. Study area

The study area is set in a lowland area in the Grand-Est region in France (Meuse). The area comprises three patches of forest of 3.44, 26.76 and 27.14 km^2, ranging from 260 m above sea level (m a.s.l.) at the bottom of large valleys, to 410 m a.s.l. on the plateau, crossed by valleys with locally steep slopes created by small streams (Fig. 1). The area is occupied by broad-leaved forests, dominated by beech stands (*Fagus sylvatica*) and mixed-forests with oak (*Quercus* spp.), hornbeam (*Carpinus betulus*), and other species (BD Forêt® v.2.0-IFN). Forest stands are owned by the State, municipalities or private bodies.

The historical occurrence of metal working activities in the 17th to early 20th centuries has been documented in the study area (Naegel, 2006; Streiff, 2015) and, along with the occurrence of charcoal kilns, several other traces are present today in the region such as forges and metal extraction sites (Arnould, 1978).

2.2. LiDAR data acquisition

The acquisition of LiDAR data was performed in two campaigns in

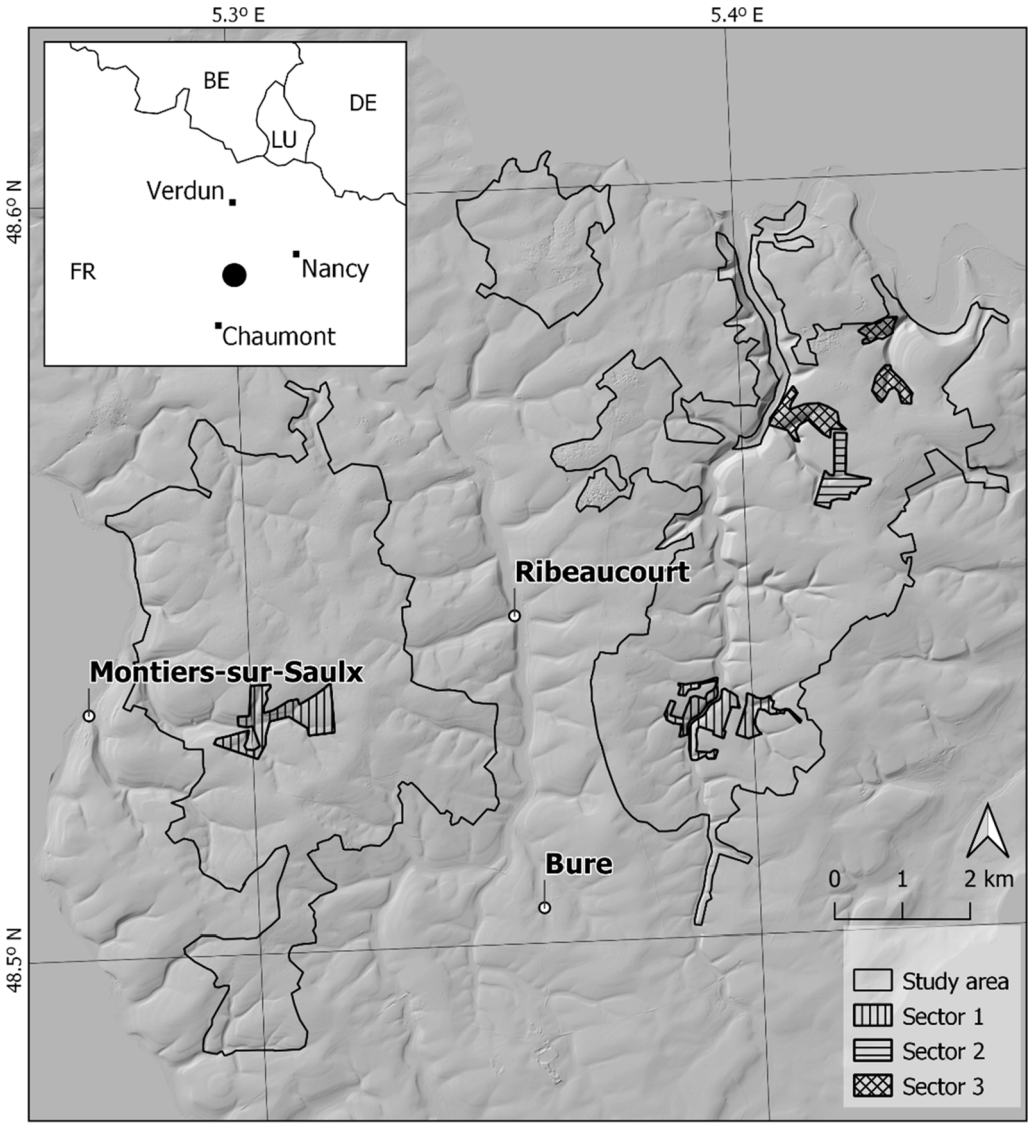

Fig. 1. Location of the study area in northeastern France lowlands, delineated by the full black line and the three sectors of field validation (in the background, hillshade representation of the DEM derived from airborne LiDAR data (restricted data access ©ANDRA)).

2009 and 2010, covering a mosaic of urban areas, agricultural fields and forests, across 230 km^2 (overlap of 60%) and an additional flight was performed in woodland areas (overlap of 20%).

The acquisition was done when broadleaved trees had shed their leaves to limit the influence of the tree canopy on the quality of the data. Individual images (1000 x 1000 pixels, 500 x 500 m) were produced, with a resolution of 4.5 points.m^{-2} and an altitudinal precision of 8 cm, resulting in the Digital Elevation Model (DEM; pixel side: 50 cm) used in this study.

From the DEM, slope-derived images (using the "Slope" tool in the "Raster terrain analysis" processing toolbox in QGIS 3.10) were also produced to help the on-screen inventory (Štular et al., 2012). When undisturbed, kilns have a characteristic outline (Bonhage et al., 2020; Hirsch et al., 2020; Ludemman and Nelle, 2002; Schneider et al., 2015) that can be recognized in the images by a ring-like boundary (Fig. 2b) or as an interruption of slope (Fig. 2d).

2.3. On-screen inventory

The on-screen inventory of kilns in the DEM was performed for each tile from the wooded areas (500 x 500 m, n = 342) comparing both hillshade (altitude 45.00°; azimuth 0.00°) and slope-derived images at a scale of 1:375. The combination of these two sets of pictures provided a complementary approach for on-screen avoiding the limitations of applying one method only. Each tile was surveyed following fictive lines in west-east and north–south directions to obtain redundant coverage in different orientations and to avoid missing areas in the images. Every time a potential kiln was found, a new point was added to the point layer.

2.4. Automatic detection inventory

For the automatic detection, TensorFlow (Abadi et al., 2016) Object Detection API, a widely used API, with several available pre-trained models was chosen. Among the available architectures, a Faster R-CNN with a Resnet 50 backbone was selected, because it is one of the smallest of the available models that have proven to be efficient at detecting small objects (Nguyen et al., 2020). Small object detection is a known limitation of object-detection architectures. Indeed, the size of a kiln is on the order of magnitude of 40 pixels depending on the DEM resolution, which is considered a small object for an object-detection task.

The initial model was trained on the Ms COCO Dataset (Lin et al., 2014) and fine-tuned on the on-screen inventory. The initial model being trained on RGB images, we first had to transform our DEM into RGB images. For this, the DEM was split with a 300 × 300 pixels sliding window, with a stride of 100 to perform data augmentation. The resulting float images were converted into RGB images with a jet colormap encoding to minimize loss of information. Then, the geographic coordinates of the on-screen detected kilns were converted into pixel coordinates in those images, and a 40 × 40 pixels bounding-box around those points was labelled as a kiln. Finally, the dataset obtained was composed of 2828 images and 5824 bounding-boxes.

Then, the dataset was split into three: training set, evaluation set, and test set. The splitting was not random because of the data augmentation technique used: a same kiln would have appeared in different sets if the images were randomly sampled.

Several parameters were tested to fine-tune the detector. The best performing ones were selected based on its results on the evaluation set, on COCO metrics. Those metrics are the standard when comparing object detectors performances. The parameters selected were as follows: the training was done on 60,000 steps, with a momentum optimizer and

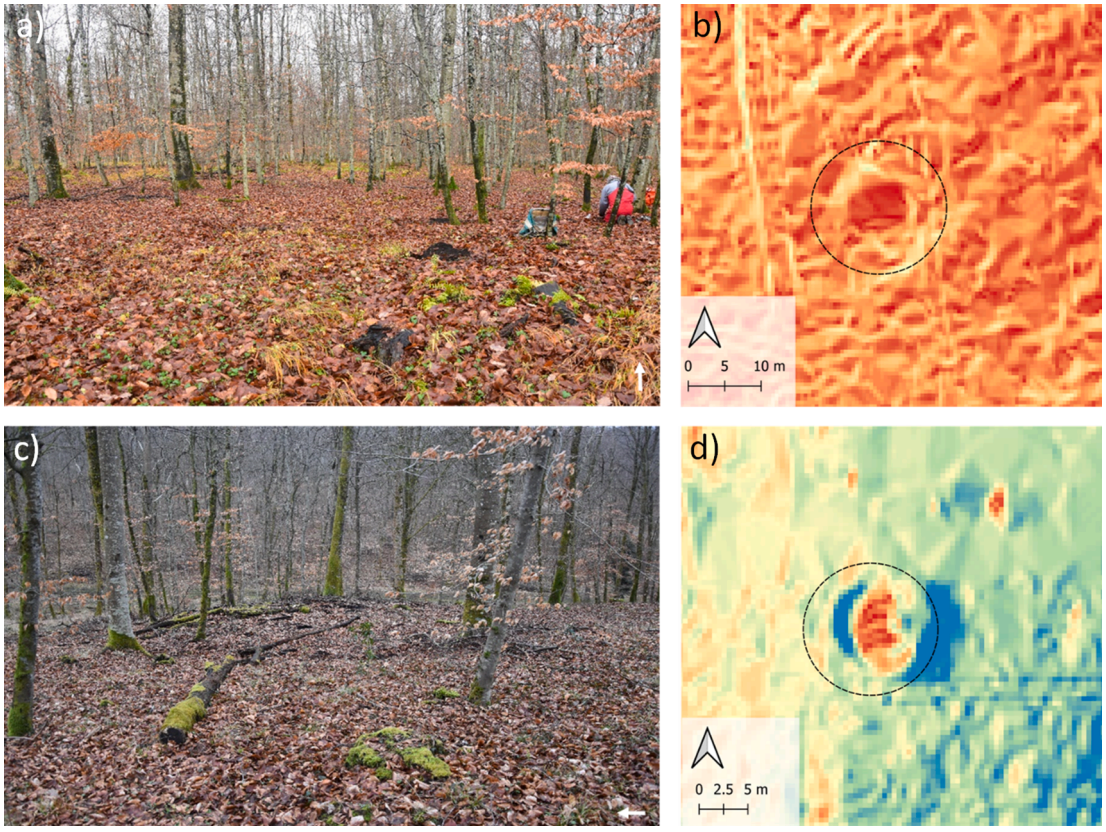

Fig. 2. Examples of charcoal kilns in the study area in contrasting slopes: a) charcoal kiln in a flat area, b) corresponding representation on a slope-derived LiDAR image, c) aspect of a charcoal kiln in a steep area, d) corresponding representation on a slope-derived LiDAR image.

an initial learning rate of 3e-04, dropped every 10,000 steps by factor of 10. Since the bounding boxes in the dataset have a fixed size of 40 × 40 pixels, this same size was used in the Region Proposal Network: the grid anchor generator parameters for height and width were 40 and the first stage features stride of the extractor was eight. The following data augmentation options were selected: random horizontal flip, random vertical flip and random rotation of 90 degrees The original images created were not resized during training.

Finally, an interface with the trained model was run on the test set and we obtained the detections: a list of detected kiln bounding-boxes in the test set images (Fig. 3).

Usually in object detection, the standard metrics are the COCO metrics: the Average Precision and the Average Recall on some specific IoU (Intersection over Union). Although those metrics were used to select the parameters to train the model, this was not how the performance of the algorithm was evaluated. The parameters of interested were Recall and Precision. Recall is related to how good the network is capable of detecting the features and Precision points to how accurate its detections are. These parameters are calculated as follows:

$$Recall = \frac{true\ positive}{true\ positive\ +\ false\ positive}$$

$$Precision = \frac{true\ positive}{true\ positive\ +\ false\ positive}$$

Thus, the higher the Recall, the less charcoal kilns are missed during the detection and the higher the Precision, the lower is the false positive occurrence. The output of the detector (the bounding boxes) was not directly used, but the centers of those boxes, converted into geographic coordinates. Thus, if an actual kiln center is within a 10 m range from the detection, it was a match.

2.5. Field validation of the inventories

Both on-screen and automatic detection inventories were validated using field-derived inventories. This is a crucial analytical step since specific landforms, such as rock slabs or fallen trees, might cause erroneous detections of kilns in the images. For the validation, 838.5 ha were prospected in three different sectors of the study area (Fig. 1).

In these sectors, several field validation protocols were used to assess possible detection biases. A first sector of 115 ha was prospected according on the basis of previously on-screen detected (OSD) kilns. Each OSD kiln of that sector was checked one by one in the field by the presence/absence of a charcoal-rich soil layer on site. That check provided "OSD-validated" or "OSD-false positive" kilns. On the tracks between each kiln, if an additional kiln, not previously detected was found, it was recorded and added to inventory as "field detected".

A second sector of 33.5 ha was specifically prospected as it corresponds to a zone with very low OSD rate. The survey was done systematically, following the limits of the forest parcel as a frame, a straight line was followed by individuals 20 to 25 m apart, and for every 8 to 12 m a surveying pit was dug to search for traces of charcoal kilns. Once found, additional kilns were added to the digital inventory as "field detected", similarly to what was done in the first sector.

The third prospected sector, covering 690 ha, corresponds to a part of the testing surface of the automatic detection (AD) on which the kilns were also OSD. Each detected kiln by both AD and/or OSD in that sector was checked and finally recorded as "OSD-validated", "AD-validated", "OSD&AD-validated", "OSD-false positive", "AD-false positive" or "OSD&AD-false positive". Also in that sector, if an additional kiln was found on the tracks between each kiln, detected neither by OSD nor by AD, it was recorded and added to inventory as "field detected".

The overall workflow of the detection and quantification is summarized in Fig. 4.

2.6. Analysis of kilns inventories and spatial distribution

Analysis were done to compare the two methods of kiln detection to field prospection in a selected sector of the study area where both methods were available. In addition to computing the error rate of each method, we also sought a relationship between topographical variables and the efficiency of the methods according to six possibilities ("field detected", "false positive on OSD", "false positive on AD", "OSD validation", "AD validation" or "OSD&AD validation"). This dataset was analyzed by a partial least square discriminant analysis (plsda, MixOmics package, (Rohart et al., 2017)). Discriminant analysis is a supervised method that aims to separate individuals according to a qualitative variable, and to identify the independent variables that drive this separation. Between-group differences were then assessed with a permutation test (Westerhuis et al., 2008).

Then, an analysis was performed to assess the spatial distribution patterns of the inventoried kilns. These variables were socio-

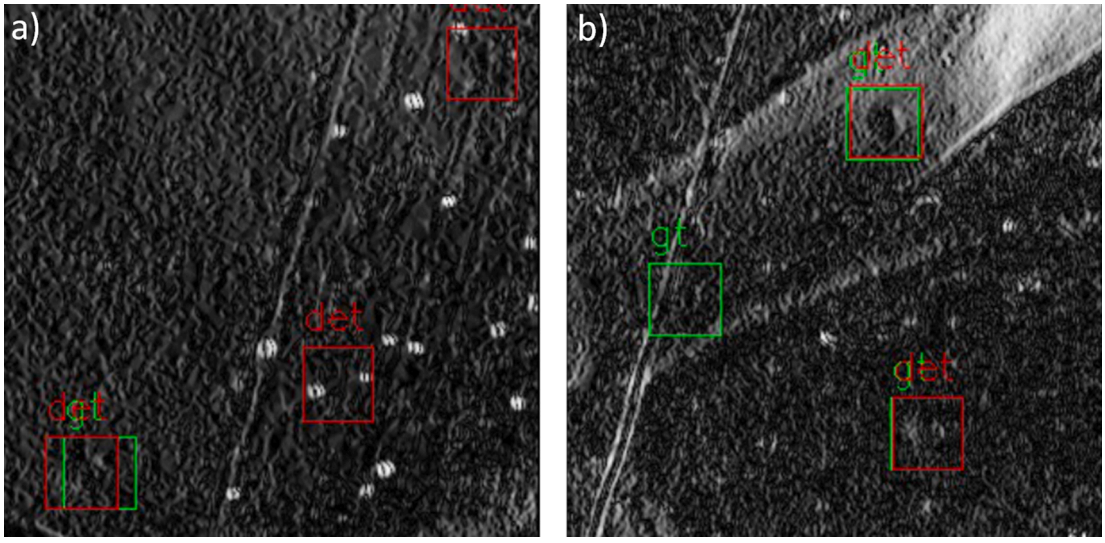

Fig. 3. Example of an area with automatic detection. The network predictions are in red ("det") and the on-screen detected data (ground truth) are in green ("gt"): a) two predictions labelled as false positive that may potentially be actual kilns (i.e. true positive); b) one missed detection (false negative). The input images in our detector are the DEM encoded in jet (these examples are filtered images for visualization purposes). (For interpretation of the references to colour in this figure legend, the reader is referred to the web version of this article.)

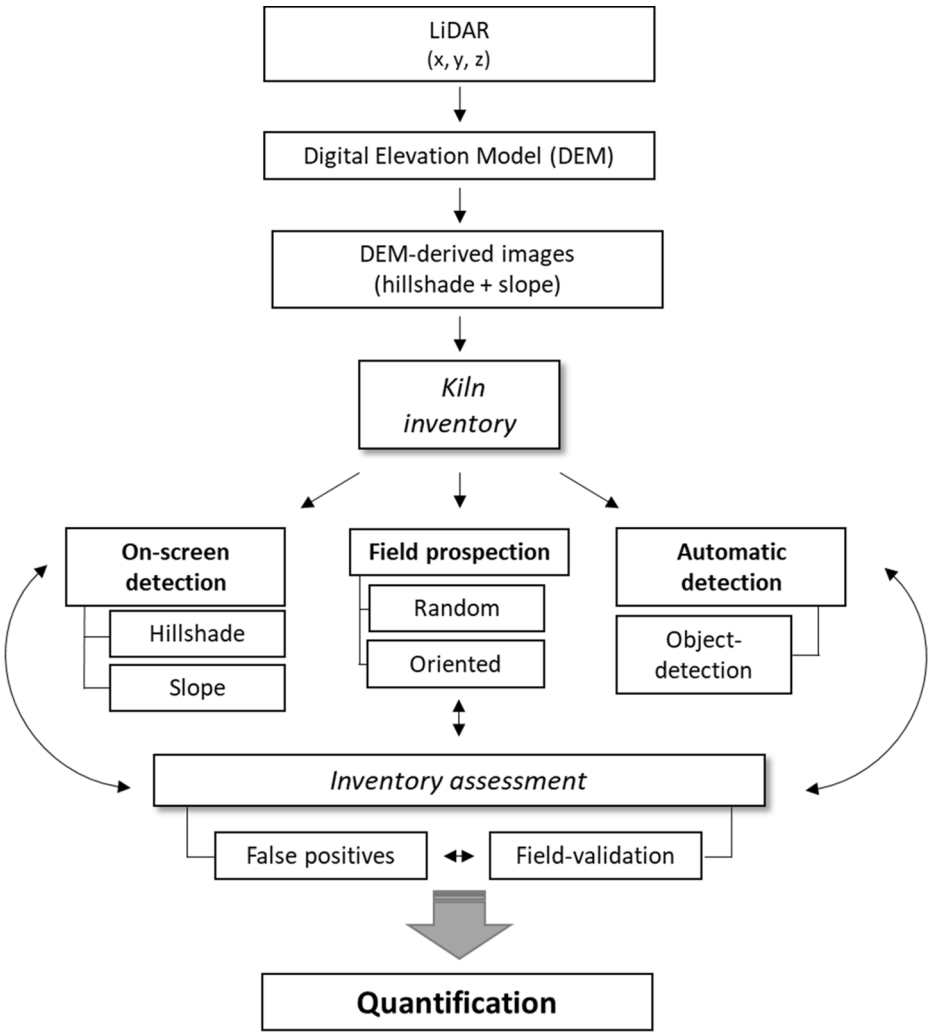

Fig. 4. Schematic summary of the for charcoal kiln quantification.

environmental territorial attributes selected among available datasets for the study area and from the GIS datasets (with Zonal Statistics tool in QGIS 3.10; Table 1). Among the available datasets, these variables were selected because they appeared relevant to explain variations in charcoal kilns' distribution.

Three grid datasets (of 125, 250 and 500 m side) were generated to explore commonalities between charcoal kiln distributions. To identify the spatial distribution patterns of kilns according to the selected socio-environmental variables, a multiple correspondence analysis (MCA) was performed with the ade4 package (Dray & Dufour, 2007) in RStudio (R Core Team, 2000; RStudio Team, 2016). This analysis allows to consider both qualitative and quantitative data from the selected socio-environmental variables. For this, the continuous variables (mean elevation, standard deviation in elevation and mean slope) needed to be transformed into qualitative variables. For aspect (i.e., exposure), eight classes were defined (following the directions of the compass) and, for slope, two classes were designated (flat and steep, <5% and >5%, respectively). The MCA was, then, applied on each grid size, to define (1) if identified patterns changed according to the scale of observation and (2) the most relevant grid size to describe kiln density patterns.

Finally, using the optimal grid size identified, the mean number of charcoal kilns was computed and the variance of charcoal kiln number across all squares for each level of the variables related to elevation and slope. Then, the variance/mean ratio was used to define whether the distribution pattern of kilns is uniform (ratio < 1), random (ratio $= 1$) or aggregated (ratio > 1).

Table 1
Socio-environmental attributes used for kiln distribution analyses.

Variable	Support	Categories	Source
Forest ownership	Vectorial	Private, Municipal, State	ONF-carmen ©
Geology	Vectorial	Calco-magnesian, Carbonate, Silico-aluminous	RRP-GrandEst, 2020
Dominant forest formation	Vectorial	*Abies/Picea*, Broad-leaved forest, Conifers, Douglas fir, *Fagus sylvatica, Larix, Quercus* deciduous, Mixed and No data	BD Forêt® v.2.0-IFN
Elevation (m a. s.l.)	Raster (DEM)	275–300, 300–325, 325–350, 350–375, 375–400	LiDAR image
Slope (%)	Raster	Flat: <5%, Steep: >5%	Derived from the LiDAR image
Aspect/ Exposure (°)	Raster	N, NE, E, SE, S, SW, W, NW	Derived from the LiDAR image

3. Results

3.1. Kiln inventories

3.1.1. On-screen detection

The on-screen inventory retrieved a total of 2641 potential kilns in

the study area (5730 ha; Table 2). The density of charcoal kilns from the on-screen inventory was 0.46 kilns.ha^{-1} and the mean distance between potential kilns was 54.7 m. The comparative analysis of the distribution of the kilns according to socio-environmental territorial attributes showed that kilns in State-owned forests represented almost half of the detections, of which 58% were positioned in areas where the slope is <5%. Regarding exposure, no kiln was found to be facing north, and the lowest detection numbers occurred in the NW and NE exposures, despite all directions representing an equivalent area. In terms of elevation, low numbers of charcoal kilns were detected in both lower (275–300 m a.s.l.) and higher (375–400 m a.s.l.) altitudinal ranges, however these were not the intervals with the lowest density observed. The three main geological types of the study area were not equally represented in terms of areas, although the density of kiln detections was similar in carbonate and silico-aluminous soils (0.46 and 0.49 kilns.ha^{-1}, respectively). Finally, areas whose present-day dominant forest cover is dominated by *Fagus sylvatica* (beech) and broad-leaved forests accounted for more than 90% of kiln detections. Low detection values in "*Larix*," "*Abies/Picea*" or "Conifers" areas, showed a high density biased by the small area of occupation of these categories that are sparsely represented in the area.

The MCA allowed to draw some trends between grid characteristics and charcoal kiln abundance. MCA results from the OSD were similar on the 125 m and 250 m grid sizes and the same trends could be seen on the 500 m grid size, but with lower accuracy. The 250 m-size grid (Fig. 5) was thus chosen as the optimal size to investigate commonalities between charcoal kilns since it allowed to better distinguish the trends. Kiln number decreases along the F2 axis (vertical), with the highest number of kilns in the lower part of the factorial plane. The factorial planes for the other variables help to understand this gradient. The grids with the highest number of kilns were associated with areas with slope steeper than 5% and with State-owned parcels that occupy the same position in the bi-dimensional space. Concerning elevation, the plateau areas had the lowest number of kilns per grid, while grids with a mean elevation between 300 and 340 m had the highest number of kilns. The lowest areas (below 300 m) also had a high number of kilns. However, such grids are rare (7% of the 1174 grids), and may be not representative of the global pattern. For the other variables, no clear pattern could be detected.

3.1.2. Automatic detection

The automatic detection was performed on a test area covering 951 ha where 342 kilns were detected (Table 2, Fig. 3), with a density of 0.36 kilns.ha^{-1}, the mean distance between the detected features being 48.4 m. The number of kilns detected in municipality-owned forests was larger, in part due to the larger area that investigated. Density trends related to forest area ownership are comparable for the two methodologies implemented. Areas with a slope above 5% accounted for almost 60% of the detections, in contrast to the trends found when using OSD. Lower number of kilns were detected in the lowest and highest altitudinal intervals ranges, despite the latter range representing the largest area under study (402 ha and only 76 kilns detected). The geological context was only represented by the occurrence of carbonate soils. The test area where automatic detection was performed did not cover all the categories of contemporary forest cover dominant groups (five out of nine categories present). Broad-leaved and *Fagus* forest formations dominated the detection numbers in terms of both area and features detected. The MCA computed for this area failed to identify specific relationships between number of kilns and the socio-environmental variables, since the ellipses for the five modalities of this variable were superimposed.

Considering the three grid sizes analyzed, the variance/mean ratio was higher than one for each class of mean slope, mean elevation and elevation standard deviation, for OSD as well as AD, therefore, a strong aggregative distribution of kilns within the prospected area can be surmised. Focusing on the 250 m grid size with the OSD dataset (the largest one), trends could be identified, with a higher aggregation in low elevation, high slope and high standard deviation in elevation.

Table 2
Summary of the detected kilns by on-screen and automatic detection.

		On-screen detection				Automatic detection			
		n (2641)	%	Area (ha)	Density (0.46)	N (342)	%	Area (ha)	Density (0.36)
Forest ownership	State	1258	47.6	1724.8	0.73	50	14.6	107.8	0.46
	Municipal	879	33.3	2604.9	0.34	267	78.1	694.4	0.38
	Private	504	19.1	1396.3	0.36	25	7.3	148.8	0.17
Exposure	N	–	–	629.8	–	–	–	77.7	–
	NE	76	2.9	679.5	0.11	9	2.6	96.3	0.09
	E	427	16.2	768.9	0.56	69	20.2	137.7	0.50
	SE	522	19.8	881.5	0.59	80	23.4	185.6	0.43
	S	537	20.3	806.2	0.67	71	20.8	163.0	0.44
	SW	417	15.8	652.0	0.64	74	21.6	121.7	0.61
	W	567	21.5	677.8	0.84	30	8.8	95.8	0.31
	NW	95	3.6	631.1	0.15	9	2.6	73.7	0.12
Slope	Flat (<5%)	1549	58.7	2664.8	0.58	138	40.4	452.0	0.31
	Steep (>5%)	1092	41.3	3062.0	0.36	204	59.6	499.0	0.41
Elevation	[250–300[	86	3.3	159.3	0.54	6	1.8	18.6	0.32
	[300–325[	372	14.1	540.1	0.69	36	10.5	51.3	0.70
	[325–350[	971	36.8	1601.3	0.61	103	30.1	137.2	0.75
	[350–375[	962	36.4	2345.6	0.41	121	35.4	342.6	0.35
	[375–410]	250	9.5	1061.2	0.24	76	22.2	401.8	0.19
Geological context	Calco-magnesian	4	0.2	87.5	0.05	–	–	–	–
	Carbonate	1726	65.4	3767.4	0.46	342	100.0	951.0	0.36
	Silico-aluminous	911	34.5	1876.9	0.49	–	–	–	–
Dominant forest formation	*Abies/Picea*	23	0.9	30.9	0.74	–	–	–	–
	Broad-leaved forest	916	34.7	2960.0	0.31	228	66.7	629.7	0.36
	Conifers	23	0.9	23.8	0.97	–	–	5.8	–
	Douglas fir	3	0.1	24.2	0.12	–	–	–	–
	Fagus sylvatica	1483	56.2	2293.0	0.65	99	28.9	274.5	0.36
	Larix	7	0.3	4.9	1.43	–	–	–	–
	Mixed	45	1.7	171.5	0.26	10	2.9	24.1	0.41
	Quercus deciduous	81	3.1	156.3	0.52	–	–	–	–
	No Data	60	2.3	115.4	0.52	5	1.5	17.0	0.29

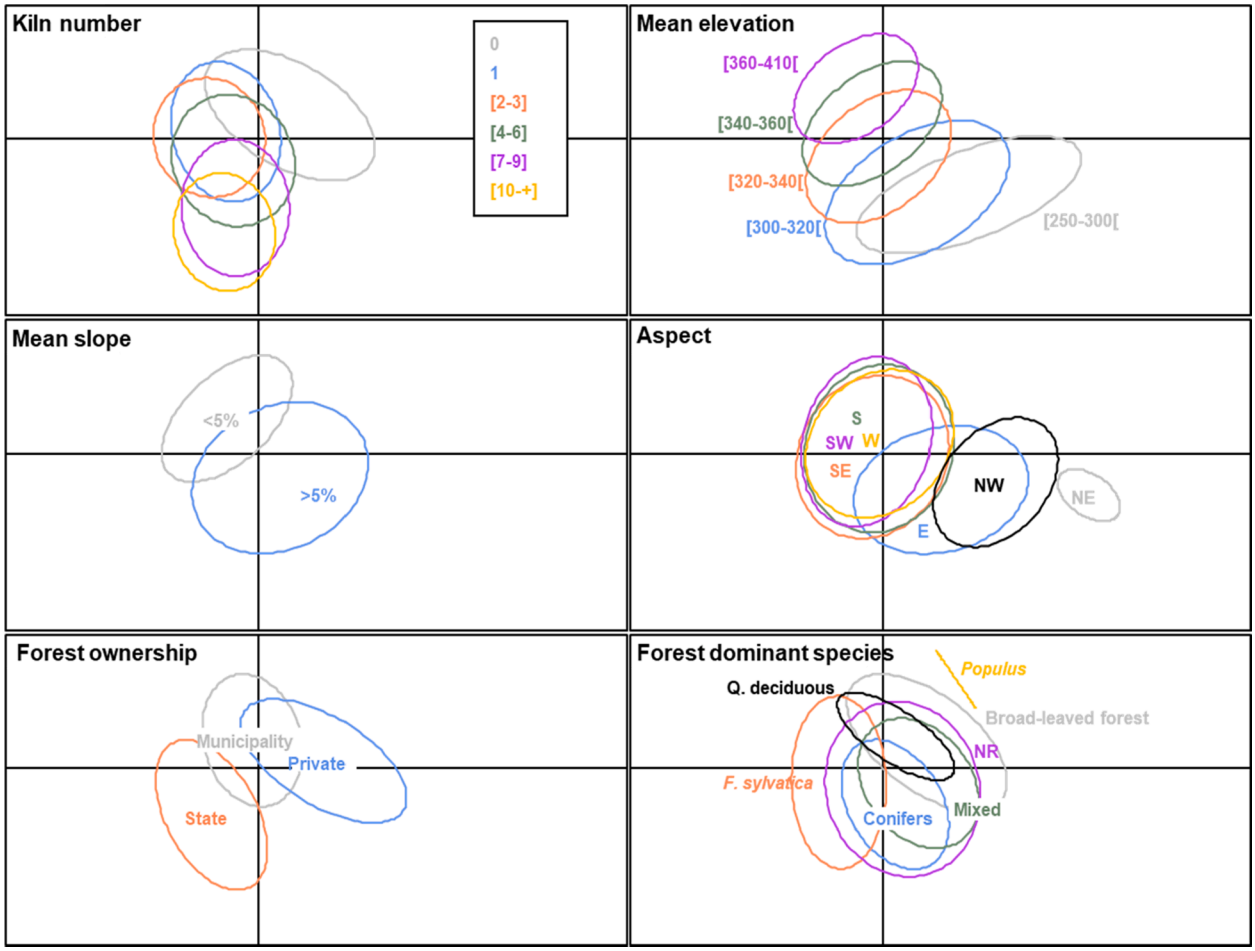

Fig. 5. MCA for on-screen detection method on the 250 m grid. Each factorial plane is built on the projection of the 1174 grids according to their topographical characteristics. Data points are then gathered according to each modality of each variable. The ellipses represent the 95% confidence interval for each modality. Modalities that occupy the same position on two different factorial planes are correlated (colors are present only to help visualization).

3.2. Inventories validation and comparison

The validation process was performed in three different sectors (Table 3, Fig. 1). Of the possible categories defined for validation, only "OSD & AD false positive" did not occur. In the first sector (with OSD only), 182 kilns out of 243 detected features were successfully field validated. Overall, in the prospected area, 61 platforms were not validated. In addition, during the validation process, 124 kilns not previously detected by OSD were added to the inventory. This first assessment retrieved a field-validated inventory of 306 kilns, hence a density of 2.66 kilns.ha^{-1}, instead of 2.11 kilns.ha^{-1} initially estimated by OSD.

Table 3
Summary of the potential charcoal kilns validated by sector (sector 1: validation in after on-screen detection only; sector 2: validation in a flat area; sector 3: validation after on-screen and automatic detection).

	Sector 1	Sector 2	Sector 3	Total
Area (ha)	115	33.5	690	838.5
Number of potential kilns detected	243	4	121	368
Density of potential kilns (kilns.ha^{-1})	2.113	0.119	0.175	0.439
OSD validated	182	0	9	191
AD validated	–	–	35	35
OSD&AD validated	–	–	53	53
OSD false positive	61	4	1	7
AD false positive	–	–	23	23
Field detected charcoal kilns	124	8	15	147
Number of kilns validated	306	8	112	426
Density of kilns validated (kilns.ha^{-1})	2.661	0.239	0.162	0.508

The second sector assessed, covering 33.5 ha, provided the OSD detection of only four features that were not field-validated charcoal kilns. Nevertheless, due to the prospection effort done in this sector, eight newly-detected charcoal kilns were detected by the presence of charcoal traces in the soil (density of 0.239 kilns.ha^{-1}).

The third sector investigated (690 ha), that combined both methods – OSD and AD – yielded 121 potential charcoal kilns. The assessment of these potential kilns returned the validation of nine kilns detected by OSD only, 35 detected by AD only, and 53 detected by both methods. False positives were also present, 23 derived from AD exclusively and one from OSD only. Similar to what occurred in the other two sectors, the inventory was enriched with 15 field-detected charcoal kilns, totalizing 112 features (density of 0.162 kilns.ha^{-1}), instead of 0.175 kilns.ha^{-1} initially estimated with OSD and AD.

In the totality of the sectors surveyed, 426 charcoal kilns were validated, 147 kilns were added after field detection only, and 89 potential kilns were not validated.

3.3. AD algorithm performance

The results of the automatic detection algorithm on the test dataset 89.69% for the Recall and 84.47% for the Precision. The algorithm was thus able to detect nearly 90% of the charcoal kilns in a given area. In 15% of the cases, the features detected were not kilns.

3.4. Validation assessment

The discriminant analysis revealed no significant differences between the six assessment types ($p = 0.05$). Hence, although the two methodologies yielded different results, the differences in accuracy and efficiency cannot be explained by the topographical variables used in these analyses.

4. Discussion

4.1. Kiln inventory

The spatial distribution of charcoal kilns detected by either OSD or AD showed strong aggregation. The aggregation measured on the basis of OSD dataset, the most consistent one, showed a trend towards a higher aggregation at low elevation, i.e., valleys, suggesting that the available space for charcoal kilns was reduced in these areas since these valleys areas are occupied by roads, paths and rivers. However, the lower aggregated pattern observed at high elevation and in smooth areas points to the difficulty in detecting charcoal kilns in such topographical features and must be taken with caution. In the flat area, the four potential charcoal kilns detected, proved to be false positives, and the newly-detected kilns in the field were not perceivable in the images. This indicates that bias was caused by methodology and not by preferences of the people when choosing the area to build a charcoal kiln or topographical constraints (Krebs et al., 2017). Lastly, aggregation tended to increase with slope, indicating that the construction of charcoal kilns demanded high efforts and, resembling the valleys, the space is limited. Indeed, despite not being identified as an important variable for kiln distribution in the study area, slope remains a relevant variable to explain the detection of charcoal kilns. Charcoal kilns need to be built on a horizontal surface to support the wood mound. On steep slopes, the presence of charcoal kilns is easily detected due to the interruption of the inclination by the platform, creating an easily spotted discontinuity (Gocel-Chalté et al., 2020; Hirsch et al., 2017; Ludemann and Nelle, 2002). However, in flat areas, insufficient heterogeneity between the charcoal kiln and its surroundings hides the presence of kilns. Moreover, the validation and prospection in the field in such areas can be made more difficult due to the presence of vegetation covering the charcoal kiln (e.g., *Hedera helix* as observed in the area) or densely-wooded areas where access is very limited or virtually impossible. The occurrence of false positives derived from the OSD in the sector 1 is, surely, overestimated due to the factors described above.

The AD method led to lower number of charcoal kilns detected and a lower frequency and density in flat areas compared to steep areas. The automatic detection rate needs to be improved to avoid biases caused insufficient data (i.e., the referential collection of ground truth data) to cover all the specificities of the charcoal kiln outlines in these areas. The quality of the template dataset provided to the algorithm to perform the AD is determinant to produce confident and reliable detections. A key step to achieve the most accurate and reliable algorithm detection is also to provide the largest possible collection of kilns contours to cope with the variability of these features (Bonhage et al., 2020; Hirsch et al., 2020). The use of template databases supported by OSD can lead to misidentification or incorrect labeling of charcoal kilns. Field validation of the detections, both by OSD and AD must be routinely performed to increase the Precision and the Recall of the detections.

Field validation of the on-screen and automatically detected charcoal kilns is an important step in the overall development of an automated methodology. Both methodologies missed the detection of charcoal platforms, and the false positives also occurred. Validation of on-screen detected kilns revealed that this method was highly precise but missed several charcoal kilns. The precision reached 98.4% (only one false positive verified) but the recall was only 63.9% suggesting that the expert was conservative in terms of which kind of landforms could potentially be kilns and only marked them when the level of confidence was high.

The performance of the AD algorithm must be looked at closely. The presence of false positives (15%) can be connected, to some extent, to labeling errors on the training dataset, and other natural or manmade structures misidentified as charcoal kilns outlines. After validation in the field, the Recall, i.e., how good the network is at finding charcoal kilns reached almost 90%, similar to other works such as Toumazet et al. (2017) in Central France where template matching methods were applied. Nevertheless, in the study cited, the precision was lower than the one achieved by the approach in this study (c. 73% versus 84% respectively), showing our method to be more robust.

Other studies have used CNNs for the detection of archaeological features (Trier et al., 2018; Bonhage et al., 2021; Trier et al., 2021) and the latter study used the same model as the present study. Trier et al. (2018; 2021) achieved similar recall than in our study, 86% or higher, reaching 96% in some cases. Nevertheless, precision was stated as being overestimated in Trier et al. (2021), at 76% dropping to 64% or even 11% depending on the area under analysis. In our study, we reached more than 84% (84.4%) precision indicating that only 15% of the detected charcoal kilns were, in fact, false positives. These values are comparable with another study by Bonhage et al. (2021) for lowland areas in North German Lowland using Mask R-CNN.

4.2. Distribution patterns

Charcoal kiln detection and inventory are important steps in the assessment of the impacts and extent of former exploitation of forest resources (Rutkiewicz et al., 2019). It is important to improve methodologies to detect these past activities, and better estimate their quantity, density and distribution. Other structures than charcoal kilns can be detected and the number of kilns can be under- or overestimated due to several factors such as image illumination, the operator's experience in performing the OSD of images or a reference database that is not sufficiently vast to perform the AD.

In this study, an area of more than 5700 ha was extensively and exhaustively examined by OSD to estimate charcoal kiln number as accurately as possible. The inventory resulting from OSD provided a density of 0.46 kilns.ha^{-1} with 2641 potential charcoal kilns detected. Deforce et al. (2013) determined a density of 0.32 charcoal kilns.ha^{-1} (49 charcoal kilns in 150 ha) by visually scanning hillshade images in an area with continuous forest cover in Northern Belgium. Schneider et al. (2020), combining several methods, performed an exhaustive mapping of charcoal kilns (>94000 charcoal kilns in, approximately, 15300 km^2) in forested areas in Germany, with densities ranging from 0.01 to 0.02 kilns.ha^{-1} to more than 2 kilns.ha^{-1}, and found that the distribution was related to former industrial activities, geology or strong relief. In our study, half of the detections were in State-owned forests, that cover only 30% of the study area, suggesting that charcoal production was actively practiced in these forests. The same trend was observed in the test area using the AD method, and densities were always higher than in municipality-owned or private areas (Table 2). Our results thus suggest that topography had a minor role in the distribution of charcoal kilns, while forest ownership status seemed to be intrinsically correlated with the presence of these structures. This correlation can be associated with the differential use of wood resources related to forest ownership and/or management practices. Wood can be immediately used as raw material for construction (e.g., oak from stands) or firewood, or used to produce charcoal. These different usages lead to different imprints in the forest, such as charcoal kilns. The low correlation of the selected variables with kiln density (or abundance), especially the variables related to topography, may give a hint that, in this area, topography did not represent a marked constraint for charcoal production, unlike in areas with more marked relief, such as the Northern Vosges (Gocel-Chalté et al., 2020) or in Hesse, Germany (Schmidt et al., 2016).

4.3. Further perspectives

The continuous acquisition of high-resolution LiDAR data presents an invaluable opportunity to explore and implement methodologies of detection and mapping on large scale. The automatic detection method used here is very flexible, allowing for reproducibility. Further perspectives after this study include the testing and evaluation of the algorithm performance in different areas and at different spatial scales with available high-resolution LiDAR data. We will also include more reliable field-validated data to increase the quality of the reference dataset used for object detection.

5. Conclusion

The detection, mapping and validation of charcoal kilns in the studied forest area revealed the occurrence of, potentially, more than 2600 charcoal kilns in an area of 57 km^2. Topographic or environmental factors were not relevant to explain the distribution of charcoal kilns in the study area, unlike socio-historical variables such as forest ownership that were found to be the relevant drivers of charcoal kiln distribution.

The conjugation of different methods allowed for a better perspective of their limitations such as operator biases during on-screen detection, insufficient ground truth data to perform AD, or the lack of representativeness in fieldwork prospection and validation. However, the results provided by AD are encouraging and the methodology developed in this work can be easily transferable to a novel environment since hand-engineering is not required to create a template model. The approach allows the user to apply the method in an area of interest without needing to invest much time to acquire specific skills. To do so, it can be mentioned that it is not necessary to pre-process the images (a DEM is sufficient) or deal with data augmentation steps, since the network does it by default. The training dataset is enriched with both positive and negative examples (examples with or without kilns), leading to an increase in precision, and a more generalized method. To build on these promising results, the network can be refined in order to achieve a better performance. The development of easy and user-friendly methodologies increases our understanding of these historical activities such as charcoal production. Exhaustive charcoal kiln inventories are key to correctly gauge the extent of former historic activities impacts where most studies rely on local-scale studies.

In this study, field validation of the detections was an important step to reach better results in both metrics (Recall and Precision) and it should be implemented routinely, even in small areas.

Declaration of Competing Interest

The authors declare that they have no known competing financial interests or personal relationships that could have appeared to influence the work reported in this paper.

Acknowledgments

This work was supported partly by the French PIA project “Lorraine Université d’Excellence”, reference ANR-15-IDEX-04-LUE. The authors thank Philippe Wagner and Paul Massard for their contribution during fieldwork. The authors are also thankful to Jean-Pascal Franco from the Office National des Forêts, and the team of the Observatoire Pérenne de L’Environnement.

Credit authorship contribution statement

Cláudia Oliveira (CO) was responsible for conceptualization, writing (original draft, review and editing), data acquisition and data analysis; Stéphanie Aravecchia (SA) and Cédric Pradalier (CP) were responsible for the development and implementation of the automatic detection methodology and writing (original draft and review); Vincent Robin (VR) and Simon Devin (SD) were responsible for the supervision, conceptualization, data analysis and writing (original draft and review).

References

Abadi, M.P., Barham, J., Chen, et al., 2016. Tensorflow: A system for large-scale machine learning. In 12th {USENIX} symposium on operating systems design and implementation ({OSDI} 16), pp. 265-283.

Arnould, E., 1978. Métallurgie au bois et utilisation de la forêt. Revue Forestière Française 6, 459–477.

Bennett, R., Welham, K., Hill, R.a., Ford, A., 2012. A comparison of visualization techniques for models created from airborne laser scanned data. Archaeological Prospection 19 (1), 41–48.

Bonhage, A., Eltaher, M., Raab, T., Breuß, M., Raab, A., Schneider, A., 2021. A modified Mask region-based convolutional neural network approach for the automated detection of archaeological sites on high-resolution light detection and ranging-derived digital elevation models in the North German Lowland. Archaeological Prospection 28 (2), 177–186.

Bonhage, A., Hirsch, F., Raab, T., Schneider, A., Raab, A., Ouimet, W., 2020. Characteristics of small anthropogenic landforms resulting from historical charcoal production in western Connecticut, USA. CATENA 195, 104896. https://doi.org/10.1016/j.catena.2020.104896.

Carrari, E., Ampoorter, E., Verheyen, K., Coppi, A., Selvi, F., 2016. Former charcoal platforms in Mediterranean forest areas: a hostile microhabitat for the recolonization by woody species. iForest-Biogeosci. Forestry 10 (1), 136–144.

Challis, K., Forlin, P., Kincey, M., 2011. A generic toolkit for the visualization of archaeological features on airborne LiDAR elevation data. Archaeological Prospection 18 (4), 279–289.

Chase, A.S., Chase, D.Z., Chase, A.F., 2017. LiDAR for archaeological research and the study of historical landscapes. Sensing the Past. Springer 89–100.

Crutchley, S., Crow, P., 2010. The Light Fantastic: Using airborne lidar in archaeological survey. English Heritage Swindon.

Davis, D.S., 2019. Object-based image analysis: a review of developments and future directions of automated feature detection in landscape archaeology. Archaeological Prospection 26 (2), 155–163.

Davis, D.S., Sanger, M.C., Lipo, C.P., 2019. Automated mound detection using lidar and object-based image analysis in Beaufort County, South Carolina. Southeastern Archaeology 38 (1), 23–37.

Deforce, K., Boeren, I., Adriaenssens, S., et al., 2013. Selective woodland exploitation for charcoal production. A detailed analysis of charcoal kiln remains (ca. 1300–1900 AD) from Zoersel (northern Belgium). J. Archaeol. Sci. 40, 681–689.

Deforce, K., Groenewoudt, B., Haneca, K., 2020. 2500 years of charcoal production in the Low Countries: The chronology and typology of charcoal kilns and their relation with early iron production. Quat. Int. 593, 295–305.

Dray, S., Dufour, A.-B., 2007. The ade4 package: implementing the duality diagram for ecologists. J. Stat. Softw. 22, 1–20.

Fouédjeu, L., Paradis-Grenouillet, S., Larrieu, L., Saulnier, M., Burri, S., Py-Saragaglia, V., 2021. The socio-ecological legacies of centuries-old charcoal making practices in a mountain forest of the Northern Pyrenees. For. Ecol. Manage. 502, 119717. https://doi.org/10.1016/j.foreco.2021.119717.

Gocel-Chalté, D., Guerold, F., Knapp, H., Robin, V., 2020. Anthracological analyses of charcoal production sites at a high spatial resolution: the role of topography in the historical distribution of tree taxa in the northern Vosges mountains, France. Vegetation History Archaeobotany 29 (6), 641–655.

Hirsch, F., Schneider, A., Bonhage, A., Raab, A., Drohan, P.J., Raab, T., 2020. An initiative for a morphologic-genetic catalog of relict charcoal hearths from Central Europe. Geoarchaeology 35 (6), 974–983.

Hirsch, F., Raab, T., Ouimet, W., Dethier, D., Schneider, A., Raab, A., 2017. Soils on historic charcoal hearths: Terminology and chemical properties. Soil Sci. Soc. Am. J. 81 (6), 1427–1435.

Kokalj, Ž., Zakšek, K., Oštir, K., 2011. Application of sky-view factor for the visualisation of historic landscape features in lidar-derived relief models. Antiquity 85 (327), 263–273.

Krebs, P., Pezzatti, G.B., Stocker, M., Bürgi, M., Conedera, M., 2017. The selection of suitable sites for traditional charcoal production: ideas and practice in southern Switzerland. J. Historical Geography 57, 1–16.

Lin, T.-Y., Maire, M., Belongie, S., et al., 2014. Microsoft COCO: Common objects in context. In: European conference on computer vision. Springer, pp. 740–755.

Ludemann, T., 2003. Large-scale reconstruction of ancient forest vegetation by anthracology-a contribution from the Black Forest. Phytocoenologia 33 (4), 645–666.

Ludemann, T., 2012. Airborne laser scanning of historical wood charcoal production sites–a new tool of kiln site anthracology at the landscape level. SAGVNTVM Extra 13, 247–252.

Ludemann, T., Nelle, O., 2002. Die wälder am Schauinsland und ihre nutzung durch Bergbau und Köhlerei. Forstliche Versuchs-und Forschungsanst, Baden-Württemberg.

Ludemann, T., Michiels, H.-G., Nölken, W., 2004. Spatial patterns of past wood exploitation, natural wood supply and growth conditions: indications of natural tree species distribution by anthracological studies of charcoal-burning remains. Eur. J. Forest Res. 123 (4), 283–292.

McCoy, M.D., Asner, G.P., Graves, M.W., 2011. Airborne lidar survey of irrigated agricultural landscapes: an application of the slope contrast method. J. Archaeol. Sci. 38 (9), 2141–2154.

Naegel, A., 2006. Le départment de la Meuse (France): industrialisation entre 1790 et 1914. Nantes University.
Nelle, O., 2003. Woodland history of the last 500 years revealed by anthracological studies of charcoal kiln sites in the Bavarian Forest, Germany. Phytocoenologia 33 (4), 667–682.
Nguyen, N.-D., Do, T., Ngo, T.D., Le, D.-D., 2020. An evaluation of deep learning methods for small object detection. J. Electr. Comput. Eng. 2020, 1–18.
Pain, S., 2017. Power through the ages. Nature 551 (7682), S134–S137.
R Core Team, 2020. R: A language and environment for statistical computing. R Foundation for Statistical Computing, Vienna, Austria.
Raab, A., Takla, M., Raab, T., Nicolay, A., Schneider, A., Rösler, H., Heußner, K.-U., Bönisch, E., 2015. Pre-industrial charcoal production in Lower Lusatia (Brandenburg, Germany): Detection and evaluation of a large charcoal-burning field by combining archaeological studies, GIS-based analyses of shaded-relief maps and dendrochronological age determination. Quat. Int. 367, 111–122.
Ren, S., He, K., Girshick, R., Sun, J., 2015. Faster r-cnn: Towards real-time object detection with region proposal networks. Adv. Neural Information Processing Syst. 28, 91–99.
Rohart, F., Gautier, B., Singh, A., Lê Cao, K.-A., 2017. mixOmics: An R package for 'omics feature selection and multiple data integration. PLoS computational biology 13 (11). https://doi.org/10.1371/journal.pcbi.1005752.
Rösler, H., Bönisch, E., Schopper, F., et al., 2012. Pre-industrial charcoal production in southern Brandenburg and its impact on the environment. Landscape Archaeology between Art and Science 167–178.
RStudio Team, 2020. RStudio: Integrated Development for R. RStudio, PBC, Boston, MA http://www.rstudio.com.
Rutkiewicz, P., Malik, I., Wistuba, M., Osika, A., 2019. High concentration of charcoal hearth remains as legacy of historical ferrous metallurgy in southern Poland. Quat. Int. 512, 133–143.
Schmidt, M., Mölder, A., Schönfelder, E., Engel, F., Fortmann-Valtink, W., 2016. Charcoal kiln sites, associated landscape attributes and historic forest conditions: DTM-based investigations in Hesse (Germany). Forest Ecosyst. 3 (1) https://doi.org/10.1186/s40663-016-0067-6.
Schneider, A., Bonhage, A., Raab, A., Hirsch, F., Raab, T., 2020. Large-scale mapping of anthropogenic relief features—legacies of past forest use in two historical charcoal production areas in Germany. Geoarchaeology 35 (4), 545–561.
Schneider, A., Takla, M., Nicolay, A., Raab, A., Raab, T., 2015. A template-matching approach combining morphometric variables for automated mapping of charcoal kiln sites. Archaeological Prospection 22 (1), 45–62.
Smil, V., 2004. World history and energy. Encyclopedia of energy 6, 549–561.
Streiff, J.-P., 2015. Le fourneau et la forge de Bértheléville. Connaissance de la Meuse 118, 4–5.
Štular, B., Kokalj, Ž., Oštir, K., Nuninger, L., 2012. Visualization of Lidar-derived relief models for detection of archaeological features. J. Archaeol. Sci. 39 (11), 3354–3360.
Toumazet, J.-P., Vautier, F., Roussel, E., Dousteyssier, B., 2017. Automatic detection of complex archaeological grazing structures using airborne laser scanning data. J. Archaeological Sci.-Rep. 12, 569–579.
Trier, Ø.D., Reksten, J.H., Løseth, K., 2021. Automated mapping of cultural heritage in Norway from airborne lidar data using faster R-CNN. Int. J. Appl. Earth Obs. Geoinf. 95, 102241. https://doi.org/10.1016/j.jag.2020.102241.
Trier, Ø.D., Salberg, A.-B., Pilø, L.H., 2018. Semi-automatic mapping of charcoal kilns from airborne laser scanning data using deep learning. In CAA2016: Oceans of Data. Proceedings of the 44th Conference on Computer Applications and Quantitative Methods in Archaeology. Archaeopress Oxford, pp. 219-231.
Westerhuis, J.A., Hoefsloot, H.C.J., Smit, S., Vis, D.J., Smilde, A.K., van Velzen, E.J.J., van Duijnhoven, J.P.M., van Dorsten, F.A., 2008. Assessment of PLSDA cross validation. Metabolomics 4 (1), 81–89.